APPLIED RESEARCH

Analysis of the GGD Vibroacoustic Detector of Power Transformer Core Damage

ROBERT KRUPIŃSKI AND **EUGENIUSZ KORNATOWSKI**

Department of Signal Processing and Multimedia Engineering, West Pomeranian University of Technology, 71-126 Szczecin, Poland

Corresponding author: Robert Krupiński (rkrupinski@zut.edu.pl)

ABSTRACT Vibroacoustic diagnostics (VM–Vibroacoustic Method) is one of the methods for diagnosing the active part of power transformers. One of the recently published objective method for the detection of transformer unit core damage was based on the analysis of the statistical properties of the vibration signal registered on the surface of the tank of an unloaded transformer in the steady state of vibrations. The GGD vibroacoustic detector of power transformer core damage is based on the relative changes in vibration power as a function of frequency and the generalized Gaussian distribution (GGD). The article shows how to configure the detector in order to reduce the variance at the detector output and speed up the detection.

INDEX TERMS Vibroacoustic method, transformer core damage, generalized Gaussian distribution, estimation.

I. INTRODUCTION

Transformers are one of the most important elements of the power system. Operators are forced to take care of their technical condition due to high production and repair costs. Although the reliability of transformers is high, in the event of damage, they lead to serious technical and economic consequences. The task of preventive diagnosis is to optimize the costs associated with maintaining reliable work of transformers.

Diagnostics of power transformers is based mainly on three technologies: analysis of transformer oil properties, Frequency Response Analysis (FRA) and vibration analysis of the unit's structure using the VM method.

Changes in the properties of transformer oil provide valuable information about the technical condition of the active part of the transformer. One of the main diagnostic methods, applied and developed for many years, is non-invasive testing of transformer oil.

The gas chromatography (DGA, Dissolved Gas Analysis) is important in assessing the technical condition of the active part. DGA is based on measurements of the concentrations of key gases: hydrogen, methane, ethane, ethylene, acetylene, carbon oxides, propane, propylene, oxygen and nitrogen

The associate editor coordinating the review of this manuscript and approving it for publication was Pinjia Zhang.

[1], [2]. Unfortunately the analysis of DGA results may lead to ambiguous conclusions as to the source of the fault. This is due to the fact that gases may be generated as a result of damage to the insulation system, but also from the core and other steel elements located inside the transformer tank.

The technical condition of the windings and some core damage is also assessed using the recently introduced FRA method [3], [4]. The method is based on the relationship between the transfer function and the winding geometrical construction. If the winding geometry changes, e.g. as a result of moving a single turn, disc or a larger part of the winding, the capacitance and inductance values of the coils also change, which leads to a change in the shape of the FRA curve. At the current stage of development of this measurement method, the assessment of winding deformation is performed by visual comparison of the measured characteristics with reference curves or comparison is conducted for a given unit between curves recorded at certain time intervals. In the case of the FRA method, the assessment of the technical condition of the active part may be ambiguous. In practice, comparative analysis usually allows for the detection of significant cases of deformation. Smaller differences between the characteristics are only interpreted as the possibility of deformation, without the possibility of locating it or assessing its size. In addition to winding defects, the shape of the frequency response characteristics may also

FIGURE 1. Transformer TR-16000/110, 115/16.5 kV, 16 MVA with accelerometer sensor and recorder.

be influenced by mechanical defects of the core (partial delamination or short circuit of magnetic circuit sheets).

A very important part of transformer diagnostics are vibration measurements of its structure. Fig. 1 shows the process of recording the acceleration signal of transformer tank vibrations with an acceleration sensor attached to the tank.

Inside the transformer, electrodynamic forces and forces caused by magnetostriction act on the windings and core, causing mechanical vibrations. These vibrations are transferred to the tank surface in two ways:

1) through the transformer oil,
2) through the lid and the base, which are in direct mechanical contact with the active part.

Loosening the windings and core sheets results in the creation of harmonic frequencies recorded on the surface of the transformer tank. Measuring steady state vibrations without load can provide important information about the condition of transformer sheets fixing [5]. The direct cause of vibrations is the phenomenon of magnetostriction, which changes the geometric dimensions of a magnetic material placed in a magnetic field. The size of the magnetic field in the core located inside the winding depends on the winding supply voltage, and not on the current flowing through the windings.

The vibrations of the transformer structure recorded by the accelerometer fastened to the tank are a superposition of the mentioned vibrations of the core and windings. The latter are subject to electrodynamic forces proportional to the square of the current flowing through them [6]. The fundamental harmonic frequency of vibrations is twice the frequency of the power grid (100 Hz for a 50 Hz power supply). The analysis of the signal separately in two time intervals of steady vibrations and transient vibrations (without load) was discussed in [7]. Therefore, when analyzing the vibration signal of the transformer tank in a steady state of vibration (negligible current) and assuming a constant

voltage amplitude, diagnostic conclusions will refer solely to the mechanical condition of the core.

In most cases, VM diagnostics are based on a simple frequency spectrum analysis, and the diagnostic conclusions are subjective and depend on the expert's professional experience. Transformer diagnostics also includes vibration measurements of its structure. In general, the vibroacoustic method consists in the analysis of the recorded signal of the transformer tank vibration acceleration. Relative changes in vibration power can be used as a qualitative criterion to assess the condition of the core [8]:

$$P_r(f) = \frac{P(f, f_t)}{P(0, f_t)}, \text{ for } 0 \leqslant f \leqslant f_t, \quad (1)$$

where $P(f, f_t)$ is the power of vibration with frequency $0 \leqslant f \leqslant f_t$, $P(0, f_t)$ denotes the total vibration power and the maximum frequency $f_t = 0.5 \cdot f_s$ is related to the sampling frequency f_s. For a perfect mechanical condition and perfect vibration measurement conditions, $P_r(f)$ is as follows: $P_r(f) = 1$ for $0 \leqslant f \leqslant 100$ Hz and $P_r(f) = 0$ for $100 \text{ Hz} < f \leqslant f_t$. For $f > 100$ Hz for a 50 Hz power grid, the function's decay rate will become slower and slower as the core continues to degrade. This core quality criterion allows you to assess the core condition.

Fig. 2 presents the amplitude characteristics of the real transformer and the corresponding relative changes in vibration power. These are data for a transformer manufactured by ELTA, type TDR-16000/110 from 1977.

A detector to identify a damaged transformer based on the relative changes in vibration power was proposed in [9]. The proposed method of vibroacoustic detection of core damage, as to the principle of performing measurements (registration of vibration acceleration), does not differ from the "classic" vibroacoustic diagnosis of transformer units. However, it must be remembered that vibrations are recorded when the transformer is operating without load. In this way, the influence of the load current on the vibration signal is eliminated. In the course of further proceedings, the Fourier transform of the recorded signal is determined, and then the relative changes in the vibration power $P_r(f)$ are calculated. The measurement data processed in this way are further analyzed using the generalized Gaussian distribution (GGD). Instead of fitting a parametric model through any optimization method to transformer data, a statistical model based on transformer data was designed and GGD was applied as a statistical tool to obtain its parameters. This detector does not determine the exact type of damage, but it indicates the probability of a defect, which is extremely valuable in the diagnosis of transformers. In this way, unnecessary, in the absence of a defect, very expensive internal inspection can be avoided. Core defect detection is performed on the basis of comparative analysis, therefore it is required to build a database, which is a set of $P_r(f)$ of many transformers with the same power and similar design features.

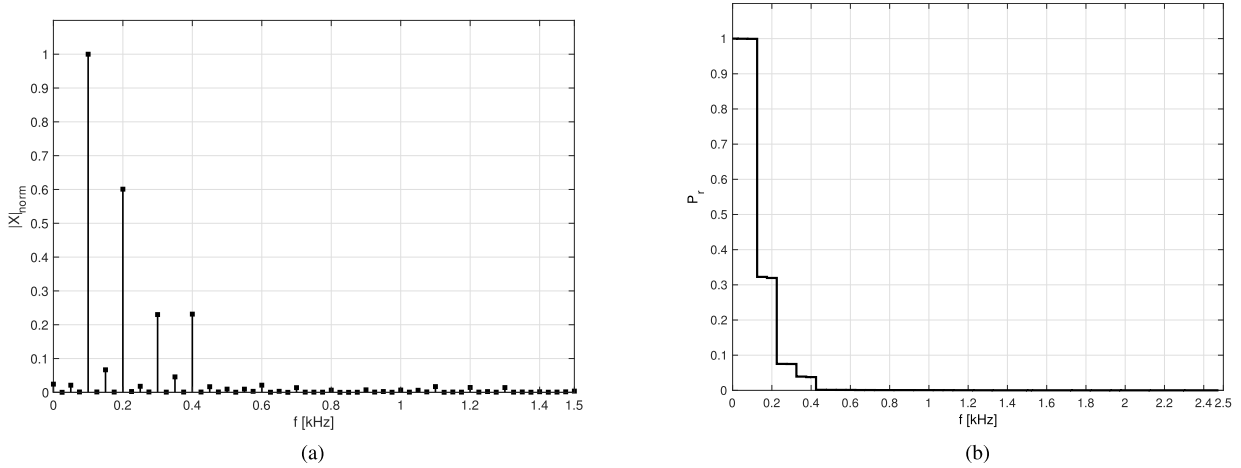Diagnostic conclusions resulting from the use of the vibroacoustic method cannot be treated as conclusively

FIGURE 2. Frequency amplitude spectra (a) and relative changes of vibration power $P_r(f)$ (b) of the real transformer.

determining the poor technical condition of the transformer. They indicate the likelihood of developing core defects. Several methods are used in parallel to diagnose transformer units (physical and chemical analysis of transformer oil, measurements of electrical parameters, FRA frequency response analysis, etc.). Only the results of all these studies lead to reliable final conclusions.

The article analyzes the statistical parameters of the detector model on its output values. Ten 16 MVA power transformers with different operating times and degrees of wear and one damaged are considered. The transformer marked as damaged was in operation the longest: it was produced in 1975. According to the operation history of this unit, it failed several times as a result of overloads. The technical condition of all considered transformers was verified by other diagnostic methods:

- Frequency Response Analysis,
- gas chromatography,
- measurements of furans contents,
- measurements of water contents,
- tests of basic electrical properties: dielectric losses coefficient (tan δ), volume resistivity, and dielectric strength.

The vibroacoustic diagnosis process itself is described in detail in a number of publications. Fig. 1 shows the course of the experiment, i.e. recording the acceleration of the tank vibrations when the transformer unit is operating without load. The subject of the article is the original concept of analyzing the recorded signal in order to formulate diagnostic conclusions.

The article is organized in the following manner. Firstly, GGD is recalled in Section II. Next, the GGD vibroacoustic detector is described in Section III. In the next Section IV, the detector is analyzed and Section V concludes the paper.

II. GENERALIZED GAUSSIAN DISTRIBUTION
One statistical model that has captured the interest of scientists is the generalized Gaussian distribution. GGD

is often used to characterize the statistical behavior of a multimedia signal. The different types of signals can be modeled in image and signal processing applications using this probability distribution. GGD also appears in the literature under other names: the exponential power distribution (EPD), the generalized error distribution (GED), the Subbotin distribution and the generalized normal distribution (GND).

The probability density function of the continuous random variable of GGD is [10]

$$f(x) = \frac{\lambda(p, \sigma) \cdot p}{2 \cdot \Gamma(\frac{1}{p})} e^{-[\lambda(p,\sigma) \cdot |x|]^p}, \qquad (2)$$

where p is the shape parameter, λ is connected to the variance of the distribution

$$\lambda(p, \sigma) = \frac{1}{\sigma} \left[\frac{\Gamma\left(\frac{3}{p}\right)}{\Gamma\left(\frac{1}{p}\right)} \right]^{0.5} \qquad (3)$$

and where σ is the standard deviation of the distribution and $\Gamma(z) = \int_0^\infty t^{z-1} e^{-t} dt, z > 0$ is the gamma function [11]. GGD covers various other distributions ranging from super-Gaussian, Gaussian to sub-Gaussian. The special cases with the exponents $p = 2$ and $p = 1$ cover the Gaussian distribution (GD) and the Laplacian distribution (LD), respectively. The GGD density function becomes a uniform distribution when $p \rightarrow \infty$. For $p \rightarrow 0$, $f(x)$ approaches an impulse function. Other values of the shape parameter p were considered in [12], [13], and [14]. The density function of GGD for different exponents is depicted in Fig. 3.

The most popular method for estimating the shape parameter of GGD is the maximum likelihood (ML) method [15]. However, this method is complex and time consuming. The
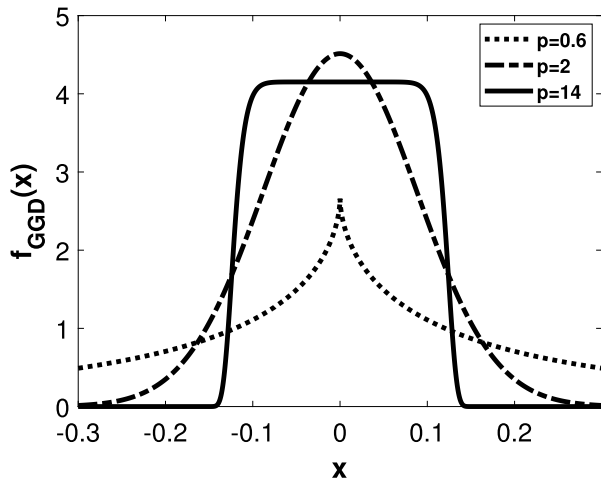
FIGURE 3. Density function of GGD with $\lambda = 8$ for three selected exponents $p = 0.6$, $p = 2$, and $p = 14$.

FIGURE 4. $f_W(w)$ - a symmetric density function for a normally working transformer and the histogram of a random variable generated with this density.

non-linear equation must be solved for p

$$C \frac{\Psi(1 + \frac{1}{p}) + \log(p)}{p^2} + \frac{1}{p^2} \log \left(\frac{1}{N} \sum_{i=1}^{N} |x_i|^p \right)$$
$$- \frac{\sum_{i=1}^{N} |x_i|^p \log(|x_i|)}{p \sum_{i=1}^{N} |x_i|^p} = 0, \quad (4)$$

where $\{x_1, x_2, \ldots, x_N\}$ is the collection of N i.i.d. zero-mean random variables and $\Psi(x) = \frac{d}{dx} \log(\Gamma(x))$ is the digamma function [11]. The maximum likelihood estimator for the λ parameter is [9]

$$\lambda = \left(\frac{N}{p \cdot \sum_{i=1}^{N} |x_i|^p} \right)^{\frac{1}{p}}. \quad (5)$$

Other methods for estimating GGD parameters have also been developed [16], [17], [18].

GGD was considered for different types of random variables: a complex valued random variable [19], [20], [21], an augmented quaternion valued random variable [22], [23], an augmented pure quaternion valued random variable [24].

In the case of a multidimensional variable, the multivariate generalized Gaussian distribution (MGGD) is used, also known as the multivariate exponential power (MEP) distribution [25], [26]. The problem of parameter estimation for such a distribution was investigated in [27], [28], and [29].

GGD has been applied in many areas: image compression [10], [30], [31], image binarization [32], [33], [34], image segmentation [35], image synthesis [36], image denoising [37], [38], image watermarking [39], [40], medical imaging [41], stereoscopic images [42], SAR images [43], radiographic images [44], texture retrieval [45], [46], [47], texture classification [48], testing adaptive filters [49], predicting failures of rotating machines [50], probabilistic classifiers [51], ultra-wide bandwidth (UWB) [52], convolutional neural networks (CNNs) [53] and detecting downhole faults [54], [55].
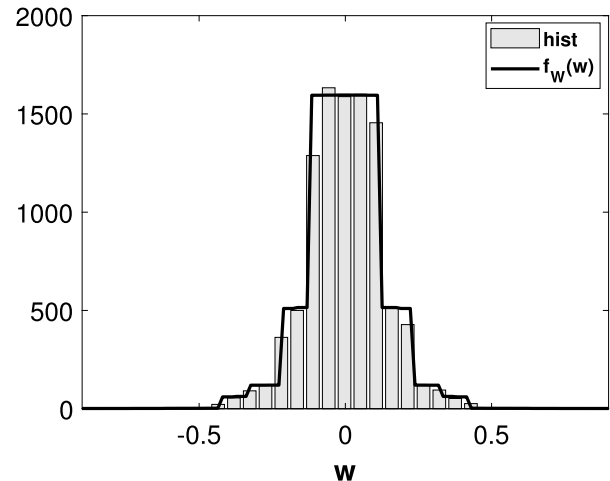
III. GGD VIBROACOUSTIC DETECTOR

The procedure for determining the output values of the detector is described in [9]. Firstly, FFT analysis of the vibroacoustic signal is performed with the determination of the relative changes in vibration power as a function of frequency $P_r(f)$ and, finally, the statistical properties of the dataset $P_r(f)$ is calculated including:

1) A cumulative distribution function dependent on transformer data is defined.
2) The random samples are generated with this distribution.

GGD is selected to approximate the distribution of the random samples in order to describe the $P_r(f)$ set. The parameters of this selected probability density function are estimated. The detector output values are the λ and p parameters of the GGD distribution. These two numerical values form the basis for the classification of the technical condition of the transformer unit core.

According to the described procedure in [9], Fig. 4 shows the probability density function for a real transformer, for which the corresponding relative changes in vibration power are shown in Fig. 2. Fig. 4 also shows the histogram of a random variable generated according to the procedure from [9]. It can be seen that the histogram coincides with the given probability density function created on the basis of the transformer data.

This histogram is also shown in Fig. 5, but this time together with the fitted approximation using GGD is presented.

Based on the ML estimation, a pair of $p = 1.1977$ and $\lambda = 7.6489$ values was determined.

IV. ANALYSIS OF THE GGD VIBROACOUSTIC DETECTOR

In the experimental part, in order to analyze the operation of the algorithm, the influence of the random sample size on the variance of the detector result was determined. As in [9], ten
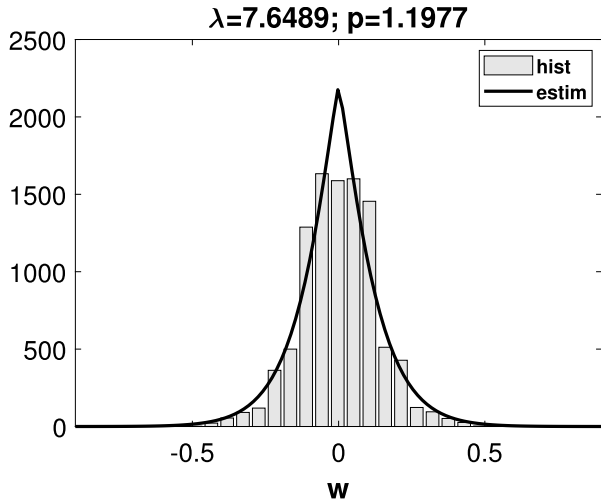
FIGURE 5. Histogram of a normally working transformer and the fitted GGD.

FIGURE 6. The average value μ_p and standard deviation σ_p of the estimated value p as the size N of the random sample increases compared to the average value μ_{p3} and standard deviation σ_{p3} of the estimated value $p3$ for the ML method and a selected transformer.

FIGURE 7. The average value μ_λ and standard deviation σ_λ of the estimated value λ as the size N of the random sample increases compared to the average value $\mu_{\lambda3}$ and standard deviation $\sigma_{\lambda3}$ of the estimated value $\lambda3$ for the ML method and a selected transformer.

TABLE 1. Average values at the detector output of the estimated values p, $p3$, λ and $\lambda3$ for 10 normally working transformers (Tr1-Tr10), a damaged one (Def) and an ideal one (Ideal) for $N = 5 \cdot 10^4$ and the ML method.

Transformer	μ_p	μ_{p3}	μ_λ	$\mu_{\lambda3}$
Tr1	1.673	1.673	4.417	4.415
Tr2	0.851	0.851	7.118	7.120
Tr3	0.852	0.851	7.115	7.119
Tr4	1.920	1.917	9.050	9.049
Tr5	0.633	0.633	13.269	13.261
Tr6	1.238	1.237	7.447	7.448
Tr7	0.637	0.637	10.220	10.216
Tr8	1.008	1.008	11.914	11.910
Tr9	1.949	1.944	5.064	5.065
Tr10	0.984	0.984	8.253	8.251
Ideal	30.000	30.000	8.009	8.009
Def	1.693	1.693	2.231	2.231

different normally functioning transformers, damaged and ideal one were explored. For 12 transformers, the relative changes of vibration power $P_r(f)$ were determined, the corresponding random samples were generated and the ML method of GGD was applied to each sequence of random samples to find the parameters p and λ, producing 12 pairs (p, λ).

In Fig. 6, for one of the correctly operating transformers, the plot shows the stabilization of the average value μ_p of the estimated value of parameter p as the size N of the random sample increases. The number of random samples N varied from $5 \cdot 10^2$ to $5 \cdot 10^4$. For each given N, the test was repeated $M = 2000$ and the mean value μ_p and standard deviation σ_p were determined. Additionally, in Fig. 6, you can see that as N increases, the standard deviation σ_p also decreases. What can be summarized is that as the random sample size N increases, the output p of the detector will on average take the value of μ_p and the variability of the result will decrease.

A similar behavior is observed at the detector output for the λ parameter (Fig. 7). For the same transformer, as the size of the random sample N increases, the mean value μ_λ of the estimated value of the λ parameter stabilizes at a certain level and the standard deviation σ_λ decreases. Which can be summed up again, as the random sample size N increases, the output λ of the detector will on average take the value of μ_λ and the variability of the result will decrease.

The conclusion is that in the detector based on the ML method, the greatest possible number of samples N should be selected. However, this results in an increase in the time needed to find a solution to the non-linear ML equation (4).

In Table 1, the results of the average estimated μ_p value of the parameter p and the average estimated μ_λ value of the λ parameter for $M = 2000$ repetitions and a relatively large random sample size of $N = 5 \cdot 10^4$ are collected. The values in the table are for 10 normally working transformers (Tr1-Tr10), a damaged one (Def) and an ideal one (Ideal).
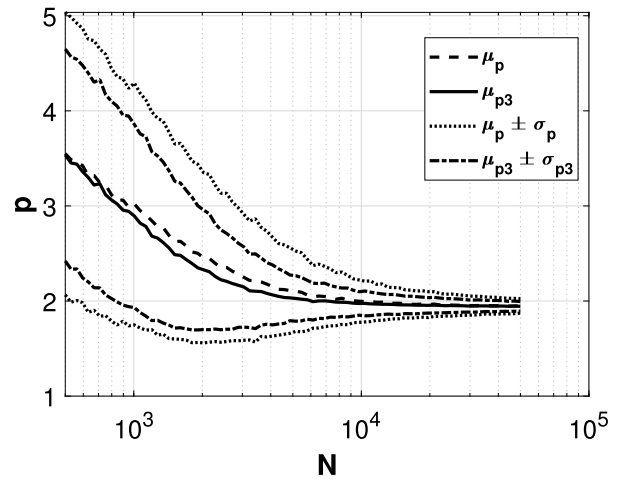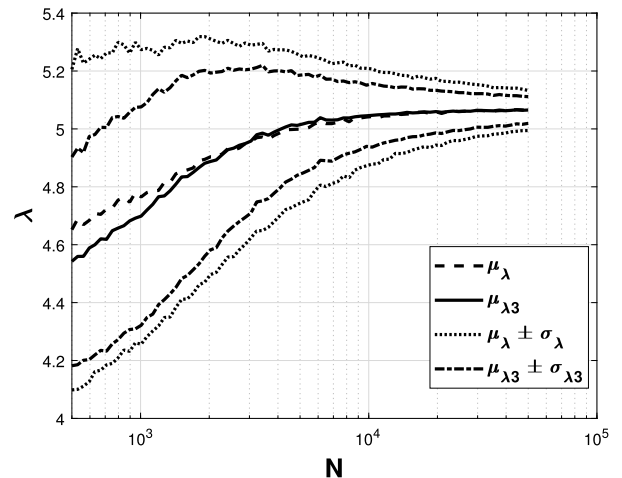
In the case of an ideal transformer, the solution of the ML equation (4) for the shape parameter p tends to infinity.
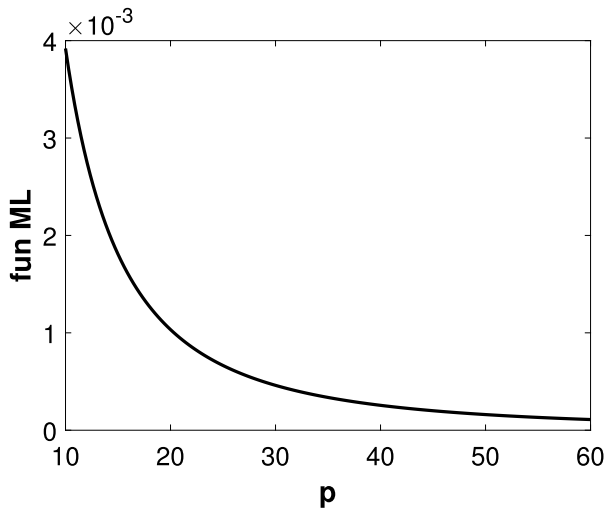
FIGURE 8. ML function (4) of an ideal transformer.

TABLE 2. Standard deviations at the detector output of the estimated values p, $p3$, λ and $\lambda 3$ for 10 normally working transformers (Tr1-Tr10), a damaged one (Def) and an ideal one (Ideal) for $N = 5 \cdot 10^4$ and the ML method.

Transformer	σ_p	σ_{p3}	σ_λ	$\sigma_{\lambda 3}$
Tr1	0.037	0.025	0.052	0.034
Tr2	0.007	0.004	0.098	0.065
Tr3	0.007	0.004	0.096	0.064
Tr4	0.086	0.059	0.165	0.114
Tr5	0.004	0.003	0.219	0.143
Tr6	0.020	0.013	0.104	0.069
Tr7	0.004	0.003	0.157	0.104
Tr8	0.013	0.009	0.175	0.118
Tr9	0.077	0.050	0.069	0.046
Tr10	0.008	0.005	0.090	0.059
Ideal	0.000	0.000	0.005	0.003
Def	0.022	0.015	0.022	0.015

Therefore, in the absence of convergence, the exponent p was limited to 30. Fig. 8 shows the ML function as it approaches 0 for increasing p values. As mentioned, this corresponds to the case when $p \to \infty$ and the GGD density function becomes a uniform distribution.

Table 2 presents the results of standard deviations σ_p and σ_λ at the detector output for the estimated p and λ parameters for a relatively large random sample of $N = 5 \cdot 10^4$ and $M = 2000$. The detector output variances, i.e. σ_p^2 and σ_λ^2, can be reduced by the following procedure. Three times the output values for the detector (calculations can be performed in parallel) p_1, p_2 and p_3 and λ_1, λ_2 and λ_3 are determined. For each set, the final result value of detector $p3$ (and $\lambda 3$) is determined by calculating the median from the values. Based on Table 2, it can be seen that the σ_{p3} and $\sigma_{\lambda 3}$ standard deviations of the $p3$ and $\lambda 3$ detector output values decreased relative to σ_p and σ_λ.

Taking into account the values in Table 1, it can be seen that the average values of the detector output for these two procedures are close: $\mu_p \approx \mu_{p3}$ and $\mu_\lambda \approx \mu_{\lambda 3}$. In Figures 6 and 7, you can compare how σ_{p3} and $\sigma_{\lambda 3}$ change for the
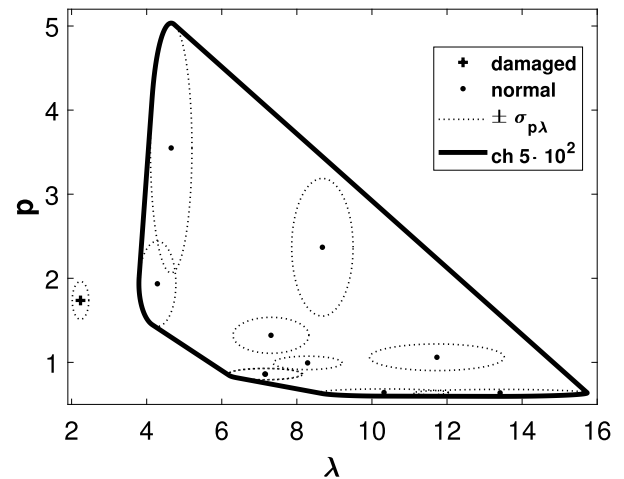

FIGURE 9. The convex hull (ch $5 \cdot 10^2$) covering correctly operating transformers (·) is separated from the area of the damaged transformer (+). The ellipses marked ($\pm \sigma_{p\lambda}$) around points (μ_p, μ_λ) are formed by the standard deviations ($\mu_p \pm \sigma_p$, $\mu_\lambda \pm \sigma_\lambda$) for $N = 5 \cdot 10^2$.

detector output pair with a variable value of N in relation to σ_p and σ_λ. It should be noted that the determined values of $p3$ and $\lambda 3$ are characterized by a smaller standard deviation.

The next conclusion is that in order to reduce the variance of the detector output values, several detector output values should be determined and the median calculated from them. Again, more solutions to the non-linear equation (4) are then needed.

In order to examine the separation of areas on the $p\lambda$ plane for correctly operating and damaged transformers, depending on the size of a random sample N, a convex hull was determined for normally operating transformers. The convex hull was constructed in such a way that it covers the points formed by the average values of the detector output (μ_p, μ_λ). The convex hull was additionally increased by the standard deviations of each point ($\mu_p \pm \sigma_p$, $\mu_\lambda \pm \sigma_\lambda$). These standard deviations were plotted as ellipses around points (μ_p, μ_λ) for different samples sizes: in Fig. 9 for $N = 5 \cdot 10^2$ and in Fig. 10 for $N = 5 \cdot 10^4$. Fig. 9 shows that the convex hull (ch $5 \cdot 10^2$) designated in this way, covering correctly operating transformers, is separated from the area of the damaged transformer (+). The faulty transformer is located leftmost on the $p\lambda$ plane with the lowest λ value. The ideal $\mu_p = 30$ transformer is located above the area and has been omitted from the diagram.

In Fig. 10 for a relatively large sample size of $N = 5 \cdot 10^4$, the standard deviations σ_p and σ_λ have decreased as shown by the smaller ellipses. In addition, the convex hull for $N = 5 \cdot 10^4$ is contained in the convex hull for $N = 5 \cdot 10^2$. Which shows that increasing the size of the random sample N increases the separation of the area containing correctly operating transformers from the area of the damaged transformer.

The computation can be sped up by reducing the sample size N at the expense of increasing the variance of the detector
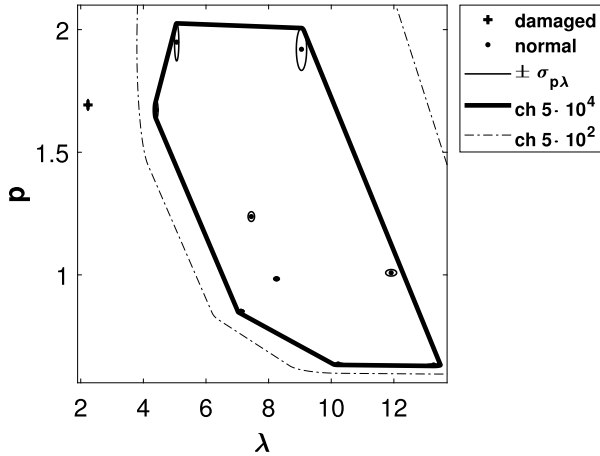
FIGURE 10. The convex hulls (ch 5 · 10^2 for $N = 5 \cdot 10^2$) and (ch 5 · 10^4 for $N = 5 \cdot 10^4$) covering correctly operating transformers (·) are separated from the area of the damaged transformer (+). The ellipses marked ($\pm\sigma_{p\lambda}$) around points (μ_p, μ_λ) are formed by the standard deviations ($\mu_p \pm \sigma_p$, $\mu_\lambda \pm \sigma_\lambda$).
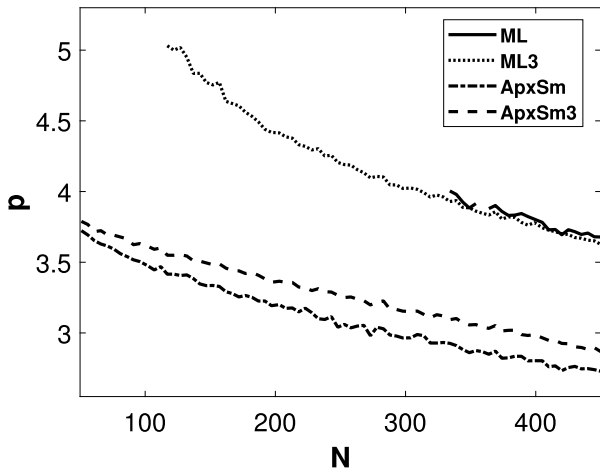

FIGURE 11. Mean values μ_p of parameter p for the ML method; mean values μ_{p3} of parameter $p3$ for the ML3 method; mean values μ_p of parameter p for the ApxSm method; mean values μ_{p3} of parameter $p3$ for the ApxSm3 method; for small values of N.

output values, but this also comes at the cost of the ML method being unsolvable. Fig. 11 presents the results of the estimation of the p parameter for the selected transformer for small values of N in the range from 51 to 450 and the number of repetitions $M = 5000$. No value in the graph means no convergence of the ML method.

Using the previously described procedure, e.g. three calculations, omitting the cases of no solution of the ML method and determining the median from the existing solutions, it is possible to increase the efficiency of determining the detector output value (ML3 in Fig. 11), but it is not always possible. Three repetitions may result in no solution too. Table 3 contains the average values for the p, $p3$, λ and $\lambda3$ parameters for the considered transformers for $N = 51$ and $M = 5000$. Improvements can be seen for $p3$ and $\lambda3$, but solutions are still missing.

TABLE 3. Average values at the detector output of the estimated values p, $p3$, λ and $\lambda3$ for 10 normally working transformers (Tr1-Tr10), a damaged one (Def) and an ideal one (Ideal) for $N = 51$ and the ML method. (-) no solution.

Transformer	μ_p	μ_{p3}	μ_λ	$\mu_{\lambda3}$
Tr1	-	3.364	-	-
Tr2	-	0.933	-	6.910
Tr3	0.955	0.930	7.580	6.893
Tr4	-	-	-	-
Tr5	0.686	0.672	14.752	13.032
Tr6	-	1.640	-	6.629
Tr7	0.703	0.676	11.217	10.079
Tr8	-	1.418	-	10.198
Tr9	-	-	-	-
Tr10	1.104	1.068	8.457	8.011
Ideal	28.329	29.498	8.101	8.060
Def	-	1.978	-	2.290

TABLE 4. Average values at the detector output of the estimated values p, $p3$, λ and $\lambda3$ for 10 normally working transformers (Tr1-Tr10), a damaged one (Def) and an ideal one (Ideal) for $N = 51$ and the ApxSm estimator.

Transformer	μ_p	μ_{p3}	μ_λ	$\mu_{\lambda3}$
Tr1	2.447	2.458	4.366	4.098
Tr2	1.044	0.999	7.115	6.552
Tr3	1.037	0.997	7.230	6.543
Tr4	3.214	3.228	9.371	8.834
Tr5	0.719	0.690	13.459	12.099
Tr6	1.651	1.618	7.128	6.613
Tr7	0.747	0.704	9.952	9.080
Tr8	1.496	1.330	11.625	10.589
Tr9	3.723	3.789	4.793	4.590
Tr10	1.203	1.174	7.901	7.406
Ideal	4.425	4.447	8.505	8.451
Def	1.912	1.884	2.380	2.226

By using the approximated fast estimator (ApxSm) from [18] one can obtain results for such small values of N. Table 4 shows that values have been determined for all transformers. This estimator does not require solving a non-linear equation, so the approximated value can be quickly determined.

Also for this estimator, by calculating the median (ApxSm3), e.g. from three estimated p values, it is possible to reduce the standard deviation of the result value. Fig. 12 shows that the σ_{p3} standard deviation of $p3$ is smaller for ApxSm3 than the σ_p standard deviation for ApxSm for the range N from 51 to 450 for the damaged transformer.

Table 5 summarizes the σ_p, σ_{p3}, σ_λ and $\sigma_{\lambda3}$ standard deviations for ApxSm and ApxSm3, which leads to the conclusion that there is a decrease in the variance at the detector output for ApxSm3 in relation to ApxSm.

As before, in Fig. 13, the calculated average values at the detector output (μ_p, μ_λ) for $N = 51$ from Table 4 have been marked on the $p\lambda$ plane with ellipses around these points showing the standard deviations ($\mu_p \pm \sigma_p$, $\mu_\lambda \pm \sigma_\lambda$) from Table 5.

A convex hull was constructed around these areas for normally operating transformers. It can be noticed that the area of the damaged transformer overlapped the convex hull of normally operating transformers. This means that there is a possibility that transformers on the border of this area may be classified in the wrong area. It also means that for a
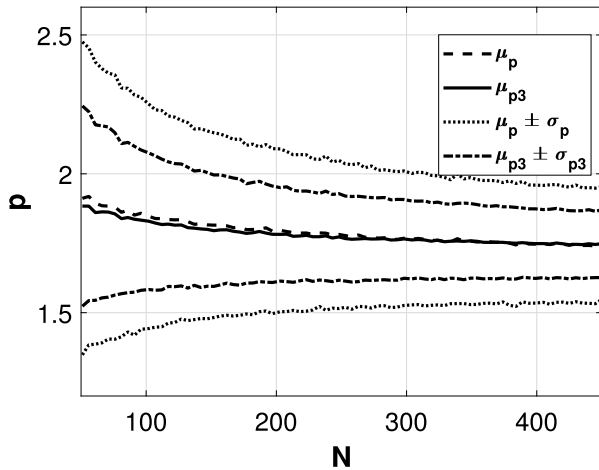
FIGURE 12. The average value μ_p and standard deviation σ_p of the estimated value p as the size N of the random sample increases compared to the average value μ_{p3} and standard deviation σ_{p3} of the estimated value $p3$ for the ApxSm estimator and a selected transformer.

TABLE 5. Standard deviations at the detector output of the estimated values p, $p3$, λ and $\lambda3$ for 10 normally working transformers (Tr1-Tr10), a damaged one (Def) and an ideal one (Ideal) for $N = 51$ and the ApxSm estimator.

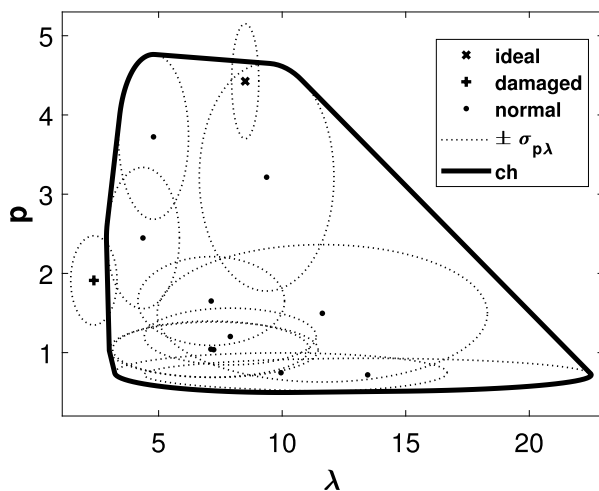| Transformer	σ_p	σ_{p3}	σ_λ	$\sigma_{\lambda3}$
Tr1	0.891	0.650	1.477	0.638
Tr2	0.354	0.243	3.974	2.273
Tr3	0.349	0.242	4.228	2.290
Tr4	1.437	1.131	2.725	1.164
Tr5	0.209	0.112	9.048	4.259
Tr6	0.560	0.339	2.969	1.426
Tr7	0.250	0.131	6.729	3.084
Tr8	0.867	0.478	6.683	3.071
Tr9	1.041	0.664	1.418	0.376
Tr10	0.358	0.239	3.479	1.990
Ideal	0.726	0.466	0.548	0.328
Def	0.563	0.361	0.936	0.429

FIGURE 13. The convex hull (ch) covering correctly operating transformers (·) overlapped the area of the damaged transformer (+). The ellipses marked ($\pm\sigma_{p\lambda}$) around points (μ_p, μ_λ) are formed by the standard deviations ($\mu_p \pm \sigma_p$, $\mu_\lambda \pm \sigma_\lambda$) for $N = 51$ and the ApxSm method. (x) - an ideal transformer.

single sample the variance of this estimator is too large. If we increase the number of trials, e.g. three times as in the case of
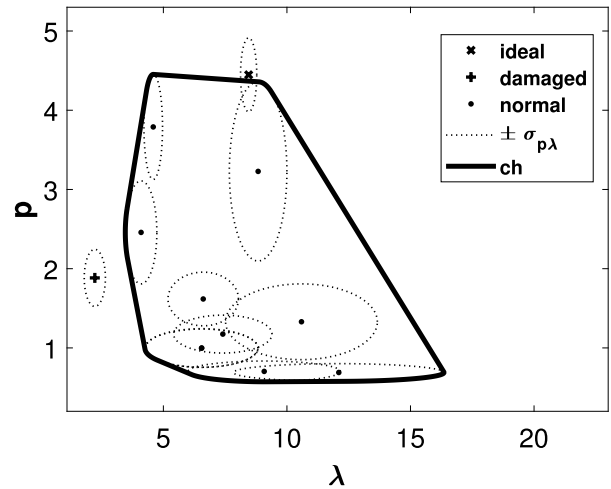

FIGURE 14. The convex hull (ch) covering correctly operating transformers (·) is separated from the area of the damaged transformer (+). The ellipses marked ($\pm\sigma_{p\lambda}$) around points (μ_{p3}, $\mu_{\lambda3}$) are formed by the standard deviations ($\mu_{p3} \pm \sigma_{p3}$, $\mu_{\lambda3} \pm \sigma_{\lambda3}$) for $N = 51$ and the ApxSm3 method. (x) - an ideal transformer.

ApxSm3, the standard deviation of the detector output values will decrease. This case is shown in Fig. 14. The average values at the detector output (μ_{p3}, $\mu_{\lambda3}$) were plotted there as well as ellipses around these points showing the standard deviations ($\mu_{p3} \pm \sigma_{p3}$, $\mu_{\lambda3} \pm \sigma_{\lambda3}$). The area indicating correctly operating transformers has shrunk and the distance from the damaged transformer area has increased. Therefore, for the ApxSm estimator, several trials should be performed and the median should be taken as the output of the detector.

As a conclusion, also for the ApxSm estimator, in order to reduce the variance of the detector output values, not just three but several detector output values should be determined and the median calculated from them.

The ApxSm estimator was not designed for large values of p, so for an ideal transformer the shape parameter p was approximated by a value of about 4.4.

Finally, it is recommended to first determine the p value quickly using the fast estimator ApxSm, and then use this p value as a starting point for the ML algorithm to accelerate convergence.

V. CONCLUSION
The article used a method of detecting defects in the mechanical structure of a power transformer core. The diagnostic process was based on a vibroacoustic study of tank vibrations in a steady state, without load, and a statistical model of GGD distribution. The calculation results related to transformers of equal power of 16 MVA with different usage periods and degrees of wear were presented.

The article has shown the influence of the variance of the maximum likelihood estimator of the GGD distribution on the pair (λ, p) constituting the output of the detector of power transformer core damage, where the reduction of the variance value is obtained by increasing the number of

random samples of the detector. The reduction of the variance of the output values can also be obtained by repeating, for example, three times the calculations and determining the median as the result value.

Speeding up the calculations can be achieved by using the approximated fast estimator [18] of GGD, but it is necessary to repeat the calculations several times and determine the median as the output value in order to reduce the variance of the output values.

An area covering correctly operating transformers has been defined, taking into account the standard deviation of the estimated values of λ and p, which has a clear separation from the area of the damaged transformer.

Imaging on the (λ, p) plane of many confirmed (preferably by internal inspection) cases of units that are functional and damaged to varying degrees is the subject of further research by the authors. This work presents the possibilities of using the GGD tool to detect possibly developing core defects. The basis of the detector's operation is comparative analysis with units of known technical condition, confirmed by diagnosis using other methods.

ACKNOWLEDGMENT

REFERENCES

[1] T. C. B. N. Assunção, J. T. Assunção, and A. D. Neto, "Classification of the power transformers using dissolved gas analysis," in *Technological Developments in Networking, Education and Automation*, K. Elleithy, T. Sobh, M. Iskander, V. Kapila, M. A. Karim, and A. Mahmood, Eds. Dordrecht, The Netherlands: Springer, 2010, pp. 225–229.

[2] I. Höhlein-Atanasova and R. Frotscher, "Carbon oxides in the interpretation of dissolved gas analysis in transformers and tap changers," *IEEE Elect. Insul. Mag.*, vol. 26, no. 6, pp. 22–26, Nov. 2010. [Online]. Available: https://ieeexplore.ieee.org/document/5599976

[3] M. H. Samimi, A. A. Shayegani Akmal, H. Mohseni, and S. Tenbohlen, "Detection of transformer mechanical deformations by comparing different FRA connections," *Int. J. Electr. Power Energy Syst.*, vol. 86, pp. 53–60, Mar. 2017. [Online]. Available: https://www.sciencedirect.com/science/article/pii/S0142061516310924

[4] *Power Transformers—Part 18: Measurement of Frequency Response*, IEC International Standard IEC 60076-18:2012, 2012.

[5] A. Secic, M. Krpan, and I. Kuzle, "Vibro-acoustic methods in the condition assessment of power transformers: A survey," *IEEE Access*, vol. 7, pp. 83915–83931, 2019.

[6] J. Shengchang, L. Yongfen, and L. Yanming, "Research on extraction technique of transformer core fundamental frequency vibration based on OLCM," *IEEE Trans. Power Del.*, vol. 21, no. 4, pp. 1981–1988, Oct. 2006.

[7] E. Kornatowski and S. Banaszak, "Diagnostics of a transformer's active part with complementary FRA and VM measurements," *IEEE Trans. Power Del.*, vol. 29, no. 3, pp. 1398–1406, Jun. 2014.

[8] E. Kornatowski, "Mechanical-condition assessment of power transformer using vibroacoustic analysis," in *Advanced Materials in Microwaves and Optics* (Key Engineering Materials), vol. 500. Wollerau, Switzerland: Trans Tech Publications, Mar. 2012, pp. 40–44.

[9] R. Krupiński and E. Kornatowski, "The use of generalized Gaussian distribution in vibroacoustic detection of power transformer core damage," *Energies*, vol. 13, no. 10, p. 2525, May 2020. [Online]. Available: https://www.mdpi.com/1996-1073/13/10/2525

[10] R. Krupiński and J. Purczyński, "Modeling the distribution of DCT coefficients for JPEG reconstruction," *Signal Process., Image Commun.*, vol. 22, no. 5, pp. 439–447, Jun. 2007. [Online]. Available: http://www.sciencedirect.com/science/article/pii/S0923596507000331

[11] F. W. J. Olver, *Asymptotics and Special Functions*. New York, NY, USA: Academic Press, 1974.

[12] F. Chapeau-Blondeau and A. Monir, "Numerical evaluation of the Lambert w function and application to generation of generalized Gaussian noise with exponent 1/2," *IEEE Trans. Signal Process.*, vol. 50, no. 9, pp. 2160–2165, Sep. 2002.

[13] R. Krupiński, "Reconstructed quantized coefficients modeled with generalized Gaussian distribution with exponent 1/3," *Image Process. Commun.*, vol. 21, no. 4, pp. 5–12, Dec. 2016.

[14] R. Krupiński, *Modeling Quantized Coefficients With Generalized Gaussian Distribution With Exponent 1/m, m=2,3* (Advances in Intelligent Systems and Computing), vol. 659. Cham, Switzerland: Springer, 2018, pp. 228–237.

[15] Y. Du, "Ein sphärisch invariantes Verbunddichtemodell für Bildsignale," *Archiv für Elektronik und Übertragungstechnik*, vol. AEÜ-45, no. 3, pp. 148–159, May 1991.

[16] R. Krupiński and J. Purczyński, "Approximated fast estimator for the shape parameter of generalized Gaussian distribution," *Signal Process.*, vol. 86, no. 2, pp. 205–211, Feb. 2006. [Online]. Available: http://www.sciencedirect.com/science/article/pii/S016516840500143X

[17] R. Krupiński, "Modified moment method estimator for the shape parameter of generalized Gaussian distribution for a small sample size," in *Computer Information Systems and Industrial Management* (Lecture Notes in Computer Science), vol. 8104, K. Saeed, R. Chaki, A. Cortesi, and S. Wierzchoń, Eds. Berlin, Germany: Springer, 2013, pp. 420–429.

[18] R. Krupiński, "Approximated fast estimator for the shape parameter of generalized Gaussian distribution for a small sample size," *Bull. Polish Acad. Sci. Tech. Sci.*, vol. 63, no. 2, pp. 405–411, Jun. 2015.

[19] M. Novey, T. Adali, and A. Roy, "A complex generalized Gaussian distribution—Characterization, generation, and estimation," *IEEE Trans. Signal Process.*, vol. 58, no. 3, pp. 1427–1433, Mar. 2010.

[20] M. Novey, T. Adali, and A. Roy, "Circularity and gaussianity detection using the complex generalized Gaussian distribution," *IEEE Signal Process. Lett.*, vol. 16, no. 11, pp. 993–996, Nov. 2009.

[21] M. S. Greco, S. Fortunati, and F. Gini, "Naive, robust or fully-adaptive: An estimation problem for CES distributions," in *Proc. IEEE 8th Sensor Array Multichannel Signal Process. Workshop (SAM)*, Jun. 2014, pp. 457–460.

[22] R. Krupiński, "Generating augmented quaternion random variable with generalized Gaussian distribution," *IEEE Access*, vol. 6, pp. 34608–34615, 2018.

[23] D. Venkatraman, V. V. Reddy, and A. W. H. Khong, "On the use of the quaternion generalized Gaussian distribution for footstep detection," in *Proc. IEEE Int. Conf. Acoust., Speech Signal Process.*, May 2013, pp. 6521–6525.

[24] R. Krupiński, "Generalized Gaussian distribution with augmented pure quaternion random variable," in *Proc. 27th Int. Conf. Methods Models Autom. Robot. (MMAR)*, Miedzyzdroje, Poland, Aug. 2023, pp. 45–50.

[25] E. Gómez, M. A. Gomez-Viilegas, and J. M. Marín, "A multivariate generalization of the power exponential family of distributions," *Commun. Statist. Theory Methods*, vol. 27, no. 3, pp. 589–600, Jan. 1998, doi: 10.1080/03610929808832115.

[26] J. K. Lindsey and P. J. Lindsey, "Multivariate distributions with correlation matrices for nonlinear repeated measurements," *Comput. Statist. Data Anal.*, vol. 50, no. 3, pp. 720–732, Feb. 2006. [Online]. Available: https://www.sciencedirect.com/science/article/pii/S0167947304002944

[27] F. Pascal, L. Bombrun, J.-Y. Tourneret, and Y. Berthoumieu, "Parameter estimation for multivariate generalized Gaussian distributions," *IEEE Trans. Signal Process.*, vol. 61, no. 23, pp. 5960–5971, Dec. 2013.

[28] N. Ouzir, F. Pascal, and J.-C. Pesquet, "Convex parameter estimation of perturbed multivariate generalized Gaussian distributions," 2023, *arXiv:2312.07479*.

[29] Z. Boukouvalas, S. Said, L. Bombrun, Y. Berthoumieu, and T. Adali, "A new Riemannian averaged fixed-point algorithm for MGGD parameter estimation," *IEEE Signal Process. Lett.*, vol. 22, no. 12, pp. 2314–2318, Dec. 2015.

[30] R. Krupiński and P. Mazurek, "Discrete Laplace estimator with a variable moment order for the modified image reconstruction," in *Proc. ICSES Int. Conf. Signals Electron. Circuits*, Sep. 2010, pp. 143–146. [Online]. Available: https://ieeexplore.ieee.org/document/5595230

[31] S. Kasaei, M. Deriche, and B. Boashash, "A novel fingerprint image compression technique using wavelets packets and pyramid lattice vector quantization," *IEEE Trans. Image Process.*, vol. 11, no. 12, pp. 1365–1378, Dec. 2002.

[32] R. Krupiński, P. Lech, M. Tecław, and K. Okarma, "Binarization of degraded document images with generalized Gaussian distribution," in *Computational Science—ICCS 2019* (Lecture Notes in Computer Science), vol. 11540, J. M. F. Rodrigues, P. J. S. Cardoso, J. Monteiro, R. Lam, V. V. Krzhizhanovskaya, M. H. Lees, J. J. Dongarra, and P. M. Sloot, Eds. Cham, Switzerland: Springer, 2019, pp. 177–190.

[33] R. Krupiński, P. Lech, and K. Okarma, "Improved two-step binarization of degraded document images based on Gaussian mixture model," in *Computational Science—ICCS 2020* (Lecture Notes in Computer Science), vol. 12141, V. V. Krzhizhanovskaya, G. Závodszky, M. H. Lees, J. J. Dongarra, P. M. A. Sloot, S. Brissos, and J. Teixeira, Eds. Cham, Switzerland: Springer, 2020, pp. 467–480.

[34] H. Michalak, R. Krupiński, P. Lech, and K. Okarma, "Preprocessing of document images based on the GGD and GMM for binarization of degraded ancient papyri images," in *Prog. Image Process., Pattern Recognit. Commun. Syst.*, in Lecture Notes in Networks and Systems, vol. 255, M. Choraś, R. S. Choraś, M. Kurzyński, P. Trajdos, J. Pejaś, and T. Hyla, Eds. Cham, Switzerland: Springer, 2022, pp. 116–124.

[35] C. Wang, "Research of image segmentation algorithm based on wavelet transform," in *Proc. IEEE Int. Conf. Comput. Commun. (ICCC)*, Oct. 2015, pp. 156–160.

[36] C. Song, F. Li, Y. Dang, H. Gao, Z. Yan, and W. Zuo, "Structured detail enhancement for cross-modality face synthesis," *Neurocomputing*, vol. 212, pp. 107–120, Nov. 2016. [Online]. Available: http://www.sciencedirect.com/science/article/pii/S0925231216307007

[37] S. G. Chang, B. Yu, and M. Vetterli, "Adaptive wavelet thresholding for image denoising and compression," *IEEE Trans. Image Process.*, vol. 9, no. 9, pp. 1532–1546, 2000.

[38] P. Moulin and J. Liu, "Analysis of multiresolution image denoising schemes using generalized Gaussian and complexity priors," *IEEE Trans. Inf. Theory*, vol. 45, no. 3, pp. 909–919, Apr. 1999.

[39] X.-Y. Wang, X. Shen, J.-L. Tian, P.-P. Niu, and H.-Y. Yang, "Statistical image watermark decoder using high-order difference coefficients and bounded generalized Gaussian mixtures-based HMT," *Signal Process.*, vol. 192, Mar. 2022, Art. no. 108371. [Online]. Available: https://www.sciencedirect.com/science/article/pii/S0165168421004084

[40] J. Liu, "An image watermarking algorithm based on energy scheme in the wavelet transform domain," in *Proc. IEEE 3rd Int. Conf. Image, Vis. Comput. (ICIVC)*, 2018, pp. 668–672.

[41] P. A. Rodriguez, V. D. Calhoun, and T. Adalı, "De-noising, phase ambiguity correction and visualization techniques for complex-valued ICA of group fMRI data," *Pattern Recognit.*, vol. 45, no. 6, pp. 2050–2063, Jun. 2012. [Online]. Available: https://www.sciencedirect.com/science/article/pii/S0031320311002020

[42] L. Ma, X. Wang, Q. Liu, and K. N. Ngan, "Reorganized DCT-based image representation for reduced reference stereoscopic image quality assessment," *Neurocomputing*, vol. 215, pp. 21–31, Nov. 2016. [Online]. Available: http://www.sciencedirect.com/science/article/pii/S0925231216306397

[43] Y. Bazi, L. Bruzzone, and F. Melgani, "An unsupervised approach based on the generalized Gaussian model to automatic change detection in multitemporal SAR images," *IEEE Trans. Geosci. Remote Sens.*, vol. 43, no. 4, pp. 874–887, Apr. 2005.

[44] N. Nacereddine, A. B. Goumeidane, and D. Ziou, "Unsupervised weld defect classification in radiographic images using multivariate generalized Gaussian mixture model with exact computation of mean and shape parameters," *Comput. Ind.*, vol. 108, pp. 132–149, Jun. 2019. [Online]. Available: https://www.sciencedirect.com/science/article/pii/S0166361518305967

[45] M. N. Do and M. Vetterli, "Wavelet-based texture retrieval using generalized Gaussian density and kullback–Leibler distance," *IEEE Trans. Image Process.*, vol. 11, no. 2, pp. 146–158, Aug. 2002.

[46] S. K. Choy and C. S. Tong, "Statistical wavelet subband characterization based on generalized gamma density and its application in texture retrieval," *IEEE Trans. Image Process.*, vol. 19, no. 2, pp. 281–289, Feb. 2010.

[47] M. S. Allili, "Wavelet modeling using finite mixtures of generalized Gaussian distributions: Application to texture discrimination and retrieval," *IEEE Trans. Image Process.*, vol. 21, no. 4, pp. 1452–1464, Apr. 2012.

[48] S.-K. Choy and C.-S. Tong, "Supervised texture classification using characteristic generalized Gaussian density," *J. Math. Imag. Vis.*, vol. 29, no. 1, pp. 35–47, Oct. 2007.

[49] R. Krupiński, "Recursive polynomial weighted median filtering," *Signal Process.*, vol. 90, no. 11, pp. 3004–3013, Nov. 2010. [Online]. Available: http://www.sciencedirect.com/science/article/pii/S0165168410001878

[50] E. Soave, G. D'Elia, and G. Dalpiaz, "Prognostics of rotating machines through generalized Gaussian hidden Markov models," *Mech. Syst. Signal Process.*, vol. 185, Feb. 2023, Art. no. 109767. [Online]. Available: https://www.sciencedirect.com/science/article/pii/S0888327022008354

[51] G. Liu, J. Wu, and S. Zhou, "Probabilistic classifiers with a generalized Gaussian scale mixture prior," *Pattern Recognit.*, vol. 46, no. 1, pp. 332–345, Jan. 2013. [Online]. Available: https://www.sciencedirect.com/science/article/pii/S0031320312003329

[52] N. Beaulieu, H. Shao, and J. Fiorina, "P-order metric UWB receiver structures with superior performance," *IEEE Trans. Commun.*, vol. 56, no. 10, pp. 1666–1676, Oct. 2008.

[53] A. Mehrabian, M. Sabbaghian, and H. Yanikomeroglu, "CNN-based detector for spectrum sensing with general noise models," *IEEE Trans. Wireless Commun.*, vol. 22, no. 2, pp. 1235–1249, Feb. 2023.

[54] Y. Li, W. Cao, W. Hu, C. Gan, and M. Wu, "Fault detection for geological drilling processes using multivariate generalized Gaussian distribution and Kullback Leibler divergence," *IFAC-PapersOnLine*, vol. 53, no. 2, pp. 164–169, 2020. [Online]. Available: https://www.sciencedirect.com/science/article/pii/S2405896320303712

[55] Y. Li, W. Cao, W. Hu, Y. Xiong, and M. Wu, "Incipient fault detection for geological drilling processes using multivariate generalized Gaussian distributions and Kullback–Leibler divergence," *Control Eng. Pract.*, vol. 117, Dec. 2021, Art. no. 104937. [Online]. Available: https://www.sciencedirect.com/science/article/pii/S0967066121002148

ROBERT KRUPIŃSKI received the B.S. and M.S. degrees in computer engineering and the Ph.D. degree in technical sciences from Szczecin University of Technology, Poland, in 2002 and 2006, respectively.

From 2006 to 2009, he was an Assistant Professor with the Department of Signal Processing and Multimedia Engineering, Szczecin University of Technology. Since 2009, he has been an Assistant Professor with the Department of Signal Processing and Multimedia Engineering, West Pomeranian University of Technology, Szczecin, Poland. After graduation, he also worked with the IT industry. His research interests include signal and images processing and software engineering.

EUGENIUSZ KORNATOWSKI was born in Szczecin, Poland. He received the degree in automation and electrical metrology from the Faculty of Electrical Engineering, Szczecin University of Technology, Szczecin, in 1981, the Ph.D. degree from Szczecin University of Technology, in 1987, and the Habilitation degree in vibroacoustic diagnostics of transformers from the Faculty of Electrical Engineering, West Pomeranian University of Technology, Szczecin, in 2019.

Currently, he is a Professor with the Department of Signal Processing and Multimedia Engineering, Faculty of Electrical Engineering, West Pomeranian University of Technology. He has been actively involved in research and development work for many years, cooperating with the ABB Research Center, Kraków, and a member of the Expert Group, OBRE Energy Research and Development Center, Piekary Śląskie. His scientific achievements include over 120 scientific articles and three implemented patents. His research interests include digital signal processing and its interdisciplinary application, in particular in sound engineering, audio technology, and vibroacoustics.

• • •